Dielectric and electrical properties of hexagonal $BaTi_{0.5}Co_{0.5}O_3$ ceramic with NTC effect

K. Samuvel[1], K. Ramachandran[1]*, V. Ratchagar[1], and G. Ravi[2]

[1]*Department of Physics, Faculty of Engineering and Technology, Vadapalani Campus, SRM University, Chennai 600026, Tamilnadu, India*
[2]*Department of Physics, Faculty of Science and Humanity, Dr. Pauls Nagar, Vanur Taluk, Villupuram 605109, Tamilnadu, India*

*Corresponding author: Tel.: (+91) 9790834728; Fax: (044) 43969957; E-mail: kaviramach76@gmail.com

Received: 10 March 2016, Revised: 30 September 2016 and Accepted: 01 October 2016

DOI: 10.5185/amp.2017/521
www.vbripress.com/amp

Abstract

Barium Titanate doped with Cobalt is known for both its electric and magnetic properties. The synthesis and characterization of Cobalt doped barium titanate; $BaTi_{1-x}Co_xO_3$(BTCO) x = 0.5was investigated with a view to understand its structural, magnetic and electrical properties. A finest possible sample of Co doped micro particles of $BaTiO_3$ (BTO) with possible tetragonal structure via a solid-state route was prepared. Prepared samples of $BaTi_{1-x}Co_xO_3$ (BTCO) were structural characterized by X-ray diffraction (XRD). The dielectric constant measurements of the samples were carried out at 1Hz to 1 MHz Vibrating Sample Magnetometer (VSM) measurements revealed the magnetic nature of Cobalt doped $BaTiO_3$. Ferroelectric hysteresis loop traced at the electric field in-between -15 to +15 (KV/cm). The relaxation phenomena that take place cane be attributable to the damping of dipole oscillator due to the application of external field. The impedance measurements were done up to 473 K in order to separate grain (bulk) and grain boundary contributions. The FESEM micrographs show proper grain growth and EDAX confirmed the presence of all the elements in samples. In the present study, various electrical properties of barium titanate based ceramics were explained and examples of the relevant applications were given. Copyright © 2017 VBRI Press.

Keywords: XRD, FESEM, BDS, VSM and ferroelectric properties.

Introduction

Barium titanate ($BaTiO_3$) is one of the bestknown Perovskite ferroelectric compounds ($A^{2+}B^{4+}O_3$) that have been extensively studied [**1, 2**] due to the simplicity of its crystal structure, which can accommodate different types of dopant. This has led to the possibility of tailoring the properties [**3**] of doped $BaTiO_3$ for specific technological applications, such as capacitors, sensors with positive temperature coefficients of resistivity, piezoelectric transducers and ferroelectric thin-film memories. Because of the intrinsic capability of the Perovskite structure to host ions of different size, large dopants can be accommodated in the lattice [**1, 4**]. The mechanism of dopant incorporation into $BaTiO_3$ has been extensively investigated [**5**] and the behaviour of some transition metal ions as well as that of the larger rare earth ions has been well elucidated. The ionic radius is the main parameter that determines the substitution site [**5**]. Since its discovery in 1945, barium titanate, $BaTiO_3$ (BTO), has attracted a great deal of attention from both fundamental research and a variety of dielectrics/electro-mechanics and nonlinear optics applications [**6-8**]. This fact is due to its high dielectric constant and low dielectric loss; good piezoelectric, pyroelectric, and ferroelectric properties [**6-8**]; positive temperature coefficient(PTC) [**9, 10**]; excellent photorefractive crystals for self-pumped phase conjugation [**11**], four-wave mixing [**12**], and many other photorefractive processes [**13**]; thin film's electro-optic modulation to frequencies over 40 GHz [**14**]; etc. Moreover, BTO doped with transition metals (e.g., Mn, Co, and Fe) has been recently revealed to exhibit the so-called giant electro-strain effect [**15–17**]. Previous reports on Mn and Co implantation of $BaTiO_3$ claimed the dilution of the transition metal ions in the $BaTiO_3$ matrix and room temperature ferromagnetism [**18**]. In the present work, preparation of $BaTiO_3$ powders from mixture of $BaCO_3$, TiO_2 and Cobalt oxide treated by a high-energy ball milling process will be reported.

Experimental

In mechanical alloying technique, the stoichiometric amount of high purity $BaCO_3$, TiO_2 and Cobalt oxide powders were mixed to obtain the $BaTi_{0.5}Co_{0.5}O_3$composition (x = 0.5). The mixture was manually ground using mortar and pestle for 2 hours. The mixed powder was taken into a Silicon Nitride bowl (50 ml). In addition to the material, 5 Silicon Nitrite (10 mm diameter) balls and 10 Tungsten Carbide (5 mm

diameter) balls were taken into the bowl. The ball to material mass ratio was maintained to 5:1. The mixed powder was subjected to mechanical alloying using Fritsch Planetary Micro Mill P7 (Made in Germany) in air. The milling was continued at rotational speed 250 rpm up to 24 hours. The option was used for reversing the direction after two hours milling and the milling was stopped for every 4 hours interval for proper mixing of the alloyed powder, and to minimize the local heat generation and particle agglomeration during material synthesis. After 80 hours milling, the material of each composition was made into several pellets of 13 mm diameter by applying 4-5 tons pressure. The pellet form of 80 hours milled material is denoted as BTCO for x = 0.5 in solid state sintering route, respectively. X-ray diffractometer using CuKα radiation with the 2θ angle in the range of 20–80^{0}and step size of 0.05^0. The crystalline phase and structure of the samples were investigated using the powder X-ray diffractometer using CuKα radiation with the 2θ angle in the range of 20–80^{0}and step size of 0.05^0.The surface morphology and structural behavior of the samples were studied by field emission scanning electron microscopy (FE-SEM, Quanta 2000 model) from the mirror polished samples. Elemental analysis of the samples was carried out using Energy Dispersive analysis of X-ray (EDAX) spectrometer and X-ray diffraction measurements (XRD, PHILIPS X ' Pert) with Cu*Kα* radiation. X-ray diffraction (XRD) patterns were recorded with a Philips X-ray diffractometer using monochromatic CuKα radiation of wavelength λ = 1.54056Å from a fixed source operated at 40 kV and 30 mA. The mean sizes of crystallites (D) were calculated from the full-width at half maximum (FWHM) of the XRD peaks using Scherrer's equation [**11**]:

$$D = K \lambda / \beta \cos\theta$$

where λ(nm) represents the wavelength of the Cu Kα radiation (1.54056 Å), θ is Braggs' angle of the selected diffraction peak, β is the corrected half-width of the selected diffraction peak, and K is a geometric factor (K = 0.89 for spherical particles). The temperature-dependent dielectric measurements were carried out using the experimental set-up made by Novo-Control GmbH. This system was equipped with a Novocontrol Alpha dielectric spectrometer, having a frequency range of 10^{-1}–10^7 Hz. The Ba $Ti_{0.5}Co_{0.5}$ O_3 ceramics sample was cut from the sintered pellet, polished and Ag electrodes were painted. The temperature was controlled using the nitrogen gas cryostat, with stability higher than 0.1 K; it was changed within the range from 298 to 473K in steps of 25K and at each temperature the stabilization time was equal to 10 min. The ferroelectric properties were tested with TF Analyzer 2000, while the ferromagnetic properties were measured with a vibrating sample magnetometer (VSM, LakeShore Model 7404).

Results and discussion

The positions of the diffraction peaks as shown in **Fig. 1** confirmed that all the studied samples are mainly in BTCO hexagonal phase with a small secondary phase detected as $BaTi_{1-x}Co_xO_3$. The diffraction peaks for the $BaTi_{1-x}Co_xO_3$ phase may be due to the preparation of samples using raw Barium carbonate, Titanium dioxide and cobalt oxide. The FESEM images of the BTCO ceramics with various amount of Cobalt oxide are shown in **Fig. 2(A), (B)** and **(C)** and a summary of the elemental composition properties is given in **Table 1.**

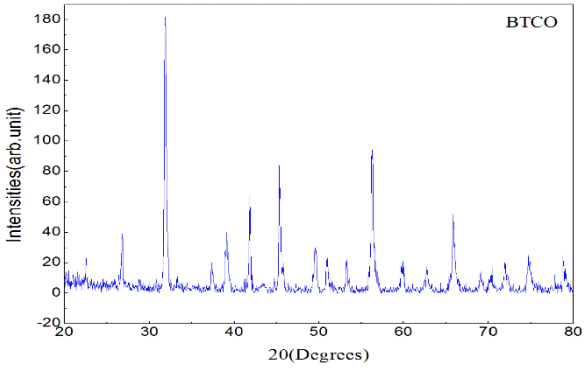

Fig. 1. X-ray powder diffraction pattern of Co doped BTO (BTCO-1000 ^{0}C) for 6 hours.

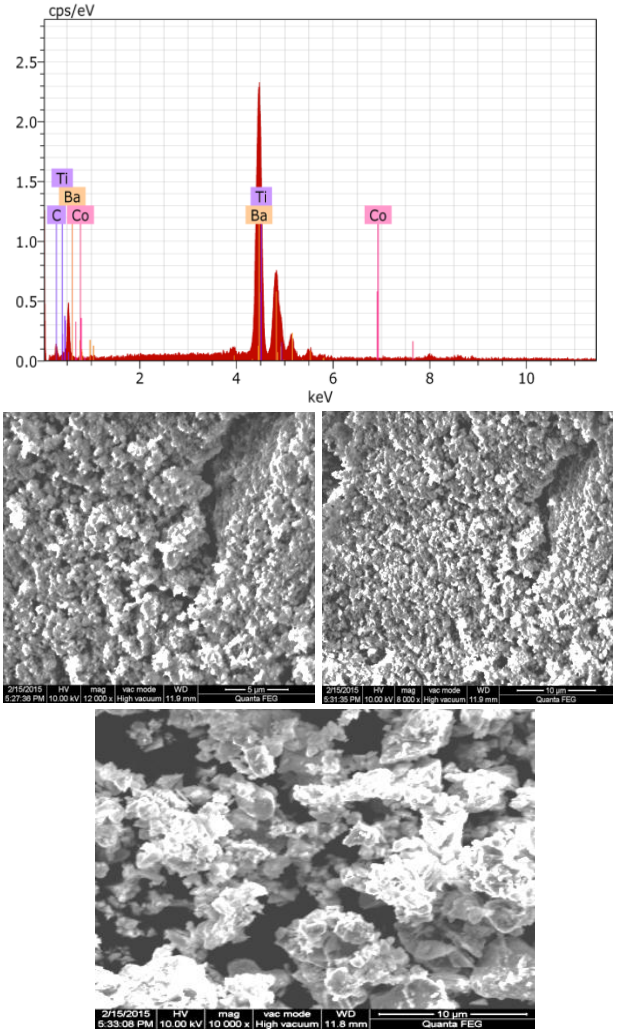

Fig. 2. FESEM images of the four-series products: 2(A)-BTCO, 2(B)-BTCO and 2(C)-BTCO ceramic sintered at room temperature with EDAX 2(D).

Table 1. Powder diffraction of BTCO-8010 doped with Co pattern.

Pos. [°2Th.]	Height [cts]	FWHM Left [°2Th.]	d-spacing [Å]	Rel. Int. [%]
26.7653	21.35	0.5904	3.33085	15.36
31.8850	138.99	0.5904	2.80675	100.00
37.4050	12.40	0.3936	2.40426	8.92
39.0742	27.70	0.3936	2.30531	19.93
41.8022	34.90	0.3936	2.16097	25.11
43.3191	3.69	0.7872	2.08875	2.66
45.4438	53.15	0.5904	1.99591	38.24
49.5692	28.73	0.3936	1.83903	20.67
51.0326	16.57	0.5904	1.78968	11.92
53.3075	13.77	0.5904	1.71855	9.91
56.3186	76.35	0.5904	1.63360	54.93
59.8521	16.11	0.3936	1.54533	11.59
62.7387	15.53	0.3936	1.48100	11.18
65.9192	35.91	0.5904	1.41704	25.84
69.1214	9.93	0.3936	1.35901	7.15
70.3422	7.31	0.5904	1.33839	5.26
71.9938	10.98	0.4920	1.31169	7.90
74.7402	19.85	0.4920	1.27016	14.28

Table 2. For BTCO (6010) Atomic percentages calculation sample.

Spectrum: training

EL	AN	Series	unn.C [wt.%]	norm.C [wt.%]	Atom. C Error [at.%]	(1 Sigma) [wt.%]
Ba	56	L-series 103.57	86.41	46.29		3.01
C	6	K-series 8.58	7.16	43.84		3.43
Ti	22	K-series 7.70	6.43	9.88		0.35
Co	27	K-series 0.00	0.00	0.00		0.00
		Total:	119.86	100.00	100.00	

The grain size of the ceramic increases significantly when the cobalt oxide is added. The micrographs show that as the Co content increases, the grain size increases with sharp grain boundaries. However, the ceramic texture become more compact as observed in the $BaTi_{0.5}Co_{0.5}O_3$sample. From **Fig. 2(D)** the EDAX images shown in demonstrate that the products are extremely relevant to that the dissolution rates of the barium and titanium precursors respectively. The approximate compositions estimated from EDS data agree well with stoichiometric chemical compositions. **Fig. 3.** The frequency (υ) dependence of real (σ'), imaginary (σ'') and resultant ac conductivity (σ) of samples has been studied in the temperature range 273–473K. The ac conductivity data of the BTCO samples are shown in **Fig. 4,** respectively. The log–log plot **Fig. 3** of the σ *(υ)* curves shows a plateau-like behaviour (i.e. nearly frequency independent) in the lower frequency regime (σ *(υ)* regime 1). The σ *(υ)* regime 1 extends to the higher frequencies with an increase in measurement temperature (*T*). Beyond the low-frequency plateau regime, the σ *(υ)* curve on the log–log scale constant increases in a linear manner σ *(υ)*. On a further increase of the measurement frequency, the σ *(υ)* curve decreasing in a relatively slow manner, suggesting a different kind of response of the bound charge carriers at higher frequencies. Electrical conductivity effects give rise to higher values of ε″ as shown in **Fig. 3**, decreasing with the increasing frequency.

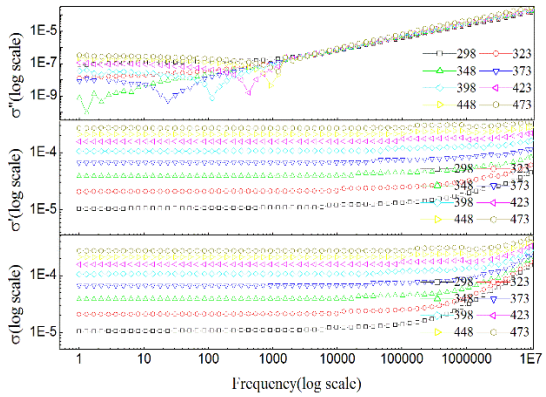

Fig. 3. Log–log scale plot of the real, imaginary and resultant ac conductivity with frequency variation at different measurement temperatures for BTCO samples.

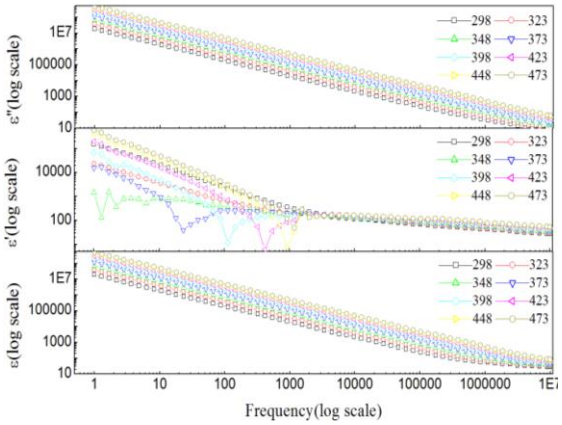

Fig. 4. The frequency dependence of the dielectric loss ε(Modulus), ε'(bottom part) and ε''(upper part) for $BaTi_{0.5}CoO_{0.5}O_3$ at different temperatures.

The relation between σ_{ac} and ε″ is given by $\sigma_{ac} = \omega\varepsilon_0\varepsilon''$. Here σ_{ac} is the ac conductivity, $\pi = \omega$ f 2 (f is the measuring frequency). The dielectric constant (ε) and dielectric losses (tan δ)of the 50 nm BT sample for several frequencies are shown in **Fig. 4** and **Fig. 8**. A diffuse phase transition with a broad maximum at 473 K was found of the maximum over the investigated range of frequencies ($1–10^6$ Hz). The maximum value of permittivity is strongly depressed in comparison to BTCO ceramics with grains≥ 1 μm. Some frequency dispersion of the maximum of tan δ can be observed in the high frequency range, as presented in the inset of **Fig. 8**. According to the dielectric data, the 38 nm BTCO system is ferroelectric at various temperature and shows a clear ferroelectric transition with a small dispersion in frequency, as in the relaxor materials. Loss tangent is the loss of electric energy in the form of heat due to the oscillation of the charge carriers. For sample the loss tangent decreases with frequency and forms a peak at a very high frequency. In order to understand the dynamics of the mobile ions in BTCO ceramics, we have plotted the angular frequency dependence of real (Z') and imaginary (Z") parts of complex electrical impedance of above ceramics in **Fig. 5** respectively at various temperatures.

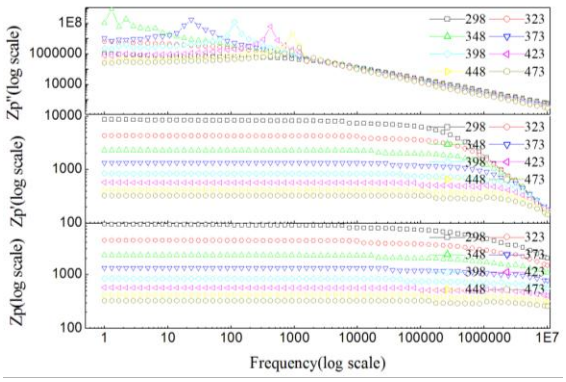

Fig. 5. The frequency dependence of the Inpedance *Zp* (Modulus), *Zp'*(bottom part) and *Zp''*(upper part) for $BaTi_{0.5}Co_{0.5}O_3$ at different temperatures.

Typical curves are observed in figures. The temperature affects strongly the magnitude of resistance. At lower temperatures, Z' and Z'' decreases monotonically with increase in frequency upto certain frequency and then becomes frequency independent. The higher values of Z' and Z'' at low frequencies and low temperatures means the polarization is larger. The temperatures where this change occurs vary in the material with frequencies. This also means that the resistive grain boundaries become conductive at these temperatures. In order to complement and verify the data obtained by fitting of the impedance complex plane plot ($Z^{/}$-$Z^{//}$), $Z^{//}$-F(Hz) and $M^{//}$-F(Hz) spectroscopic plots were used for the extraction of grain and grain boundary resistivities of the BTCO material **(Fig. 5)**.

Fig. 6 The effect of conductivity can be highly suppressed when the data is presented in the modulus representation. The electric modulus approach began when the reciprocal complex permittivity was discussed as an electrical analogue to the mechanical shear modulus [**20**]. From the physical point of view, the electrical modulus corresponds to the relaxation of the electric field in the material when the electric displacement remains constant. From the physical point of view, the electrical modulus corresponds to the relaxation of the electric field in the material when the electric displacement remains constant. Therefore, the modulus represents the real dielectric relaxation process [**21**]. The complex modulus $M^{*}(\omega)$ was introduced to describe the dielectric response of non-conducting materials. This formalism has been applied also to materials with non-zero conductivity. The usefulness of the modulus representation in the analysis of relaxation properties was demonstrated both for vitreous ionic conductors [**22**] and polycrystalline ceramics [**23**].

Fig. 7 shows the time dependence of the capacitance under at various temperatures. In the samples, the aging rate decreased with increasing Cobalt oxide content, but the change was relatively modest in the intermediate ionic radius rare-earth (Cobalt oxide)-doped samples. In contrast, the larger ionic radius rare-earth (La_2O_3, Sm_2O_3) doped samples showed a large dependence on the Co content, and the sample containing x = 0.5 stoichiometric ratio Co showed significantly large aging rate due to the grain growth.

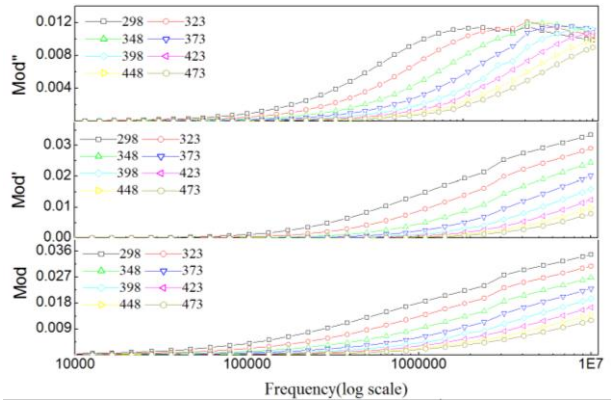

Fig. 6. The frequency dependence of the real, $M^{/}$, and imaginary, $M^{//}$, parts of the electric modulus for $BaTi_{0.5}Co_{0.5}O3$.

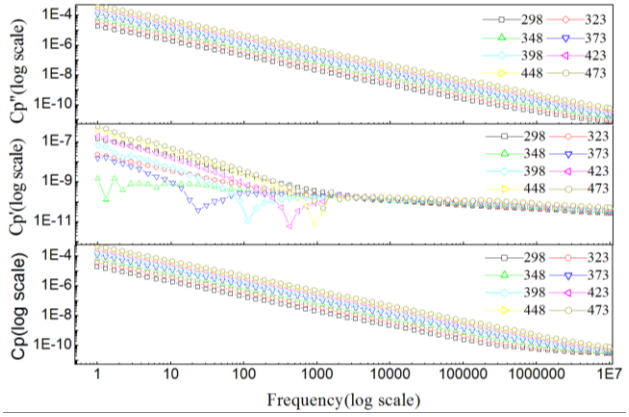

Fig. 7. The frequency dependence of the real $Cp^{/}$, and imaginary$Cp^{//}$, parts of the Capacitance for $BaTi_{0.5}Co_{0.5}O_3$.

A new behavior develops at higher frequencies and the dielectric constant becomes almost temperature independent at F= 1Hz to1MHz. The temperature dependent dielectric loss (tan δ) slowly decreases with an increase in temperature, with the exception at lower frequencies (1000 Hz) and temperatures up to 473K. Beyond this temperature, the loss registers a small increase **(Fig. 8)**.

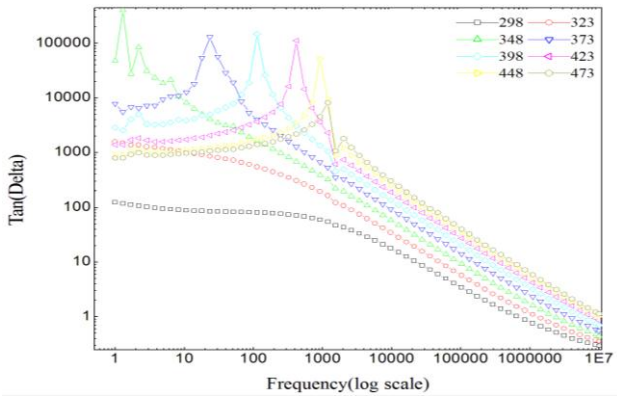

Fig. 8. Frequency dependence of loss Tangent for BTCO samples.

In dielectric materials, the defects, space charge formation, lattice distortions in the boundaries produce an absorption current, results in dielectric loss. The main source of dielectric loss in ceramic materials is photon absorption, which is associated with structural disorders such as creation of an oxygen deficiency in the material due to doping [24, 25]. **Fig. 9.** Frequency dependence of Specific resistance for BTCO samples is increased the frequency and decreased in specific resistance. We have analyzed the real ($Zs^{/}$) and imaginary ($Zs^{//}$) parts of the complex impedance of different samples using the Cole–Cole plot. **Fig. 10** shows the Cole–Cole plot at different measurement temperatures for BTCO samples, respectively. A large semi-circular arc for each temperature intersects the real (Z) axis at the lower side of the applied frequency, i.e. at a higher value of Z. For clarity, we have restricted the limit of Y and X scales. The grain boundary resistance (R_{gb}) of the sample was estimated by fitting the $Z^{/}$versus $Z^{//}$curves using a semi-circle that intersected the higher Z value, as indicated in **Fig. 10**. We noted that R_{gb} of the samples decreases with the increase in temperature, which supports the thermally activated conductivity change in the samples. **Fig. 11** shows that the $M^{//}$constant decreases with the increase of frequency. At very low frequency dipoles follow the field as the frequency increases dipoles begin to lag behind the field and $M^{/}$rapidly increases. When frequency attains a certain particular value, characteristics of the material, the dielectric constant drops (relaxation process). This is the normal behavior of dielectric material. So, the Modulus constant decreases at high frequency and vice versa. Similar behavior is also observed in the present experiment on Cobalt oxide-doped $BaTiO_3$.Broadband dielectric spectroscopy is widely used to investigate the dielectric and electric properties of ceramics. From the dielectric response one can obtain, among others, important information on the relaxation processes occurring in the system. The dielectric properties of materials can be expressed in various ways, using different representations. Although these alternative representations are equally valid [26], they may often provide new insight into the dielectric and electrical properties of materials. For example, a comparison of the complex dielectric permittivity ε^* and electric modulus M^* representation allows us to distinguish the local dielectric relaxation from long-range electrical conductivity. **Fig. 12** shows the room temperature magnetization (M) vs. applied magnetic field (H) hysteresis loops of the $BaTi_{0.5}Co_{0.5}O_3$ ceramics with Co^{3+} doping concentration x. Except for the sample with x = 0.5 at%, samples showed room temperature ferromagnetism. As shown in the upper inset of **Fig. 12,** the sample with x = 0.5 at%, however, exhibited ferromagnetism at 300 K. The lower inset of **Fig. 12** shows the dependence of the saturation magnetization (MS) and magnetic coercivities (HC) on x at room temperature. MS increased with x to reach a maximum value at about 0.32emu/g then followed by a decrease. Magnetization measurements suggest samples have a magnetic ordering at room temperature depending on the amount of x. The origin of magnetism is believed to be from Co^{3+} ion in the high spin state. Present study clearly showed that magnetism especially ferromagnetism can be induced in a ferroelectric material by appropriate selection of substituents which may find multiferroic applications.

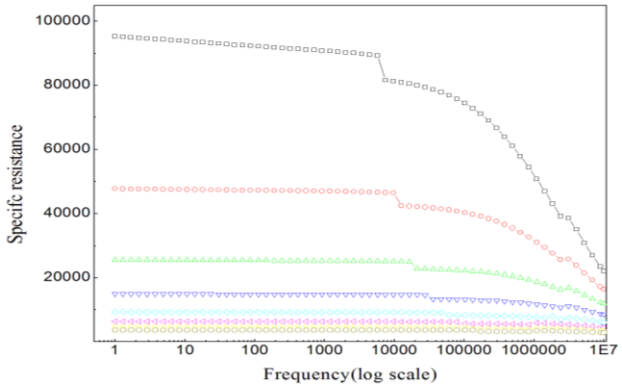

Fig. 9. Frequency dependence of Specific resistance for BTCO samples.

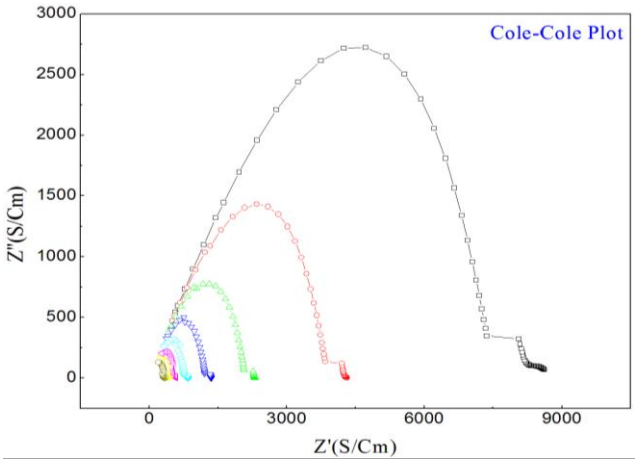

Fig. 10. Impedance Cole-Cole plot of the BTCO ceramics at various temperatures.

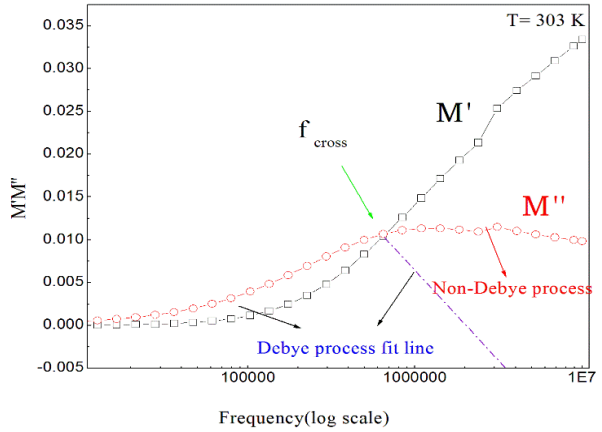

Fig. 11. Real, $M^{/}$and imaginary, $M^{//}$ part of the electric modulus versus log f obtained at a temperature T = 303 K. The position of the maximum in the $M^{//}$ curve gives the relaxation time, τM of the most prominent process. This maximum is broader than a simple Debye relaxation. The Debye-like dependence fits the low-frequency wing of $M^{//}$ as depicted by the dotted curve. The frequency of the crossing point, $f$cross is related to the dc-conductivity relaxation time, τdc(Modulus compare **Fig. 6**).

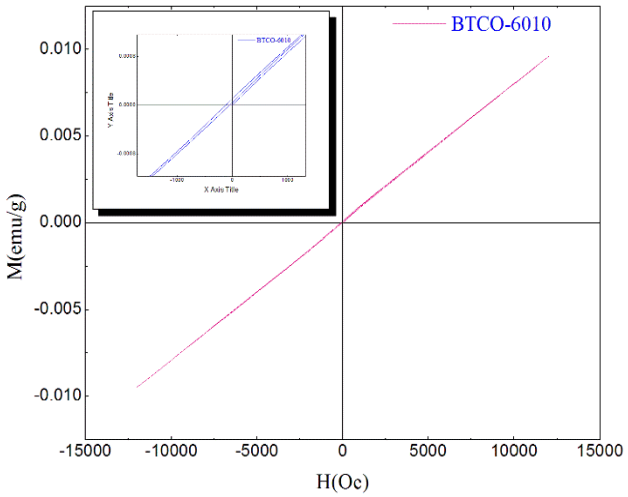

Fig. 12. Dependence of the magnetization (M) on the magnetic field intensity(H) for measured 303K (BTCO-8010) sample.

Conclusion

The system $BaTi_{1-x}Co_xO_3$ where x=0.5 is prepared by solid state reaction method. The Phase change in the crystal structure was observed with cobalt in BTCO, however a decrease in crystallite size, c/a ratio and grain size were found with cobalt doping. All the different results presented may be related to, and are explained by, the grain size and its distribution in the ceramic bulk. Cobalt doping in $BaTiO_3$ exhibit many interesting features, such as shit in transition temperature, increasing diffused phase transition and decreasing dielectric phase transition to a diffuse phase transition was observed with increasing cobalt concentrations. The dielectric study of samples poled in magnetic field suggests that Tc and maximum dielectric constant increase with increasing magnetic poling strength along with decreasing nature of diffusivity. We have studied the electrical conductivity of $BaTi_{1-x}Co_xO_3$ Ceramics with grain size in the nanometer scale. The samples showed a significant enhancement of conductivity ~10^4 times in the measurement temperature scale 298–473 K. Conductivity is fed by highly conducting grains and highly conducting grain boundaries that act as a potential barrier between two grains. The samples showed the existence of two relaxation processes in the measurement temperature scale. It is understood that the interactions between two grains or at the interfaces of grains and grain boundaries played a significant role in decreasing the activated conductivity at higher frequencies. The sample also showed a few more interesting features, e.g. ac conductivity scaling, hopping conductivity between ions and enhancement of conductivity in smaller sized grains. This work clearly identified two distinct conduction mechanisms, associated with the single domain and multi-domain states of the magnetic grains. There is a 50Kdifference in the annealing temperature scale between the transition of electrical parameters and magnetic parameters, which occurred due to the transformation of domain structure from single domain to multi-domain in the grains. Our experimental result of enhanced electrical conductivity in the single domain state of the grains could be useful in synthesizing nanoceramic based solid-state materials [**26**].

Acknowledgements

The authors convey the heartfelt gratitude to the Nanotechnology research center in SRM University. The authors would like to express their sincere thanks to the Mr. K. KUMARAVEL for the constant support. Authors also thank to the work has been permitted for instrumentation facility in Broad band dielectric/Impedance spectrometer (Novocontrol technology) and VSM, Pondicherry University (CIF).

References

1. D. Makovec, Z. Samadmija and M. Drofenik, "Effect of Copper Doping on Structural, Dielectric and DC Electrical Resistivity Properties of $BaTiO_3$,"J. Am. Ceram. Soc. 87, 1324 (2004).
2. D. Maga, P. Igor and M. Sergei,"Influence of impurities on the properties of rare-earth-doped barium-titanate ceramics", J. Mater. Chem. 10, 941 (2000).
3. A. Jana, T. K. Kundu, S. K. pradhan and D. Chakravorty, "Dielectric behavior of Fe-ion doped $BaTiO_3$ nanoparticles" J. Appl. Phys. 97 (4), 44311 (2005).
4. Z. Jin, C. Ang and Z. Yu "Incorporation of Yttrium in Barium Titanate Ceramics", J. Am. Ceram. Soc. 82(5) 1345 (1999).
5. P. Yongping, Y. Wenhu and C. Shoutian,"Influence of Rare Earths on Electric Properties and Microstructure of Barium Titanate Ceramics", J. Rare Earths. 25, 154 (2007).
6. V.P.Pavlovic1, B.D.Stojanovic2 , V.B.Pavlovic3*), Z.Marinkovic-Stanojevic2 , Lj.Živković4 , M.M.Ristic "Synthesis of BaTiO3 from a Mechanically Activated BaCO3-TiO2 System", Sci. Sinter. 40, 155 (2008); Sci. Sinter.40, 235 (2008).
7. Ha M. Nguyen, N. V. Dang, Pei-YuChuang"Tetragonal and hexagonal polymorphs of $BaTi_{1-x}Fe_xO_{3-\delta}$ multiferroics using x-ray and Raman analyses",Appl. Phys. Lett. 99, 202501 (2011).
8. F. Jona and G. Shirane, "Ferroelectric Crystals", (Dover Pulications, ICN., New York, 1993).
9. R. L. Brutchey, G. Cheng, Q. Gu, "Positive Temperature Coefficient of Resistivity in Donor-Doped $BaTiO_3$ Ceramics derived from Nanocrystals synthesized at Low Temperature", Adv. Mater. 20, 1029 (2008).
10. J. Nowotny and M. Rekas, "Defect Structure, Electrical Properties and Transport in Barium Titanate. VII. Chemical Diffusion in Nb-Doped $BaTiO_3$", Ceramics International 20, 265 (1994).
11. M. Kaczmarek and R.W. Eason, "Very-high-gain single-pass two-beam coupling in blue Rh:$BaTiO_3$", Opt. Lett. 20, 185 (1995).
12. G. N. Henderson, J. F. Walkup, and E. J. Bochove, "Optical quadratic processor using four-wave mixing in $BaTiO_3$", Opt. Lett. 14, 770 (1989).
13. P. Günter and J.-P. Huignard (edts.), "Photorefractive Materials and Their Applications"1, (Springer Science-Bussiness Media, Inc., New York , 2006).
14. P. Tang, D. Towner, T. Hamano"Electrooptic modulation up to 40 GHz in a barium titanate thin film waveguide modulator," Opt. Express 12, 5962 (2004).
15. W. Liu, W. Chen, L. Yang, "Ferroelectric aging effect in hybrid-doped BaTiO3 ceramics and the associated large recoverable electrostrain"., Appl. Phys. Lett.89, 172908 (2006).
16. X. Ren"Large electric-field-induced strain in ferroelectric crystals by point-defect-mediated reversible domain switching", Nature Mater. 3, 91 (2004).
17. X. Ren and K Otsuka"Universal Symmetry Property of Point Defects in Crystals", Phys. Rev. Lett. 85, 1016 (2000).
18. Lee J S, Khim Z G, Park Y D, Norton D P, Theodoropoulou N A, Hebard A F, Budai J D,Boatner L A, Pearton S J and Wilson R G "Magnetic properties of Co- and Mn-implanted $BaTiO_3$, $SrTiO_3$ and $KTaO_3$", Solid State Electron. 47 2225 (2003).
19. McCrum N G, Read B E and Williams G "Anelastic and Dielectric Effects in Polymeric Solids" (New York: Wiley) 1967.

20. Wagner H and RichertR "Thermally stimulated modulus relaxation in polymers: method and interpretation,"J. Polymer 38 5801(1997) Leon C, Lucia M L and Santamaria "Correlated ion hopping in single-crystal yttria-stabilized zirconia "J. Phys. Rev. B 55 882(1998).
21. Macedo P B, Moynihan C T and Bose R "The long time aspects of this correlation function, which are obtainable by bridge techniques at temperatures approaching the glass transition", Phys. Chem.Glasses13 171(1972).
22. Liu J, DuanCh-G, Yin W-G, Mei W N, Smith R W and Hardy J R,"Dielectric permittivity and electric modulus in $Bi_2Ti_4O_{11}$" J. Chem. Phys. 119 2812 (2003).
23. A.G. Belous, O.V. Ovchar, M. Valant, D. Suvorov, D. Kolar"The effect of partial isovalent substitution in the A-sublattice on MW properties of materials based on $Ba_{6-x}Ln_{8+2x/3}Ti_{18}O_{54}$ solid solutions", J. Eur. Ceram. Soc. 21, 2723(2001).
24. DalveerBindraKaur, SukhleenNarang, K. Singh"Synthesis and characterization of $Ba_{6-3x}Sm_{8+2x}Ti_{18}O_{54}$ microwave dielectric ceramics", Ceram.Int.33, 249(2007).
25. McCrum N G, Read B E and Williams G "Anelastic and Dielectric Effects in Polymeric Solids" (New York: Wiley)1967.
26. Petric A and Ling H "Electrical Conductivity and Thermal Expansion of Spinels at Elevated Temperatures" J. Am. Ceram. Soc. 90 1515(2007).

